Enhancing photocatalytic degradation of methylene blue by TiO_2-CeO_2 heterostructure under visible light irradiation

Vu Thi Nga[1], Le The Tam[2], Nguyen Hoa Du[1], Nguyen Hoang Hao[1], Le Thi Thu Hiep[3], Chu Thi Thanh Lam[3], Nguyen Thi Kim Chung[3], Nguyen Le Khanh Huyen[4], Ho Thi Van Suong[2], Nguyen Thi Quynh[1], Ho Dinh Quang[1*]

[1]Department of Chemistry, College of Education, Vinh University, Vinh City, Nghe An, Vietnam;
[2]School of Chemistry, Biology and Environment, Vinh University, Vinh City, Nghe An, Vietnam;
[3]Centre for Practice and Experiment, Vinh University, Vinh City, Nghe An, Vietnam;
[4]Phan Boi Chau High School for Gifted, Vinh City, Nghe An, Vietnam.
[*]Corresponding author: hodinhquangdhv@gmail.com
Received 14 Oct. 2023; Revised 2 Dec. 2023; Accepted 10 Feb. 2024; Published 25 Feb. 2024.
DOI: https://doi.org/10.54939/1859-1043.j.mst.93.2024.99-105

ABSTRACT

TiO_2-CeO_2 heterostructure was synthesized by a simple hydrothermal technique, with an average particle size of 21 nm, and high uniformity from the common precursors. For the characterization of the catalyst properties, the techniques of X-ray Diffraction (XRD), Fourier-Transform Infrared Spectroscopy (FTIR), and Transmission Electron Microscopes (TEM) were used. The TiO_2-CeO_2 heterostructure exhibited higher photocatalytic activity than TiO_2 in the removal of methylene blue (MB) dye under visible light irradiation. The combination of TiO_2-CeO_2 facilitated electron pathways, creating favorable conditions for efficient separation of electron-hole pairs and enhancing the photocatalytic activity of the material. The TiO_2-CeO_2 heterostructure demonstrated rapid and highly efficient photodegradation of methylene blue, achieving an 89.79% removal rate after 120 minutes of irradiation. This performance, coupled with enhanced visible light utilization, suggests wide applications in the field of photocatalysis.

Keywords: TiO_2 nanoparticles; TiO_2-CeO_2 heterostructure; Methylene blue and photocatalytic degradation.

1. INTRODUCTION

Untreated wastewater discharged by the textile industry poses a significant threat to water bodies, adversely affecting both aquatic ecosystems and human health [1]. Of particular concern is the waste from textile dyeing, as synthetic dyes, commonly used for their cost-effectiveness and durability, present challenges in degradation. The persistent color and resistance to breakdown in their waste necessitate thorough treatment before release into natural water systems. This precaution is vital, given that 1-15% of these dyes cannot be recycled and require proper disposal [2]. During the dyeing Methylene blue (MB), a prevalent textile dye, sees only 5% utilization during the dyeing process, with the remaining 95% typically discharged as challenging-to-degrade waste due to its high stability [3], addressing this waste issue is crucial. Multiple approaches, such as electrocoagulation [4], adsorption [5], electrochemical methods [6], and photocatalytic degradation [7], have been employed. Notably, photocatalytic degradation emerges as a superior choice, demonstrating the capacity to break down organic compounds into simpler and more environmentally friendly components [8].

Titanium dioxide (TiO_2) is a well-known semiconductor material frequently employed in photodegradation processes to address environmental issues. Nevertheless, TiO_2 possesses a relatively wide band gap energy of 3.28 eV, that only operates well in the UV light range (4% of solar radiation), making it less efficient for degrading organic pollutants [8]. To harness the potential of the remaining 46% of solar radiation in the visible light spectrum, efforts have been made to lower band gap energy and inhibit recombination processes. Various methods have been explored to reduce the band gap energy of TiO_2 and enhance its performance under visible light

through the creation of a coupling or heterojunction with other semiconductor materials [9]. Combining TiO_2 with various metal oxides, such as SnO_2, ZnO, WO_3, Cu_2O, CeO_2 enhances photocatalyst performance compared to using TiO_2 alone [10]. These synthesized nanomaterials exhibit broad visible light absorption, prolonged charge carrier lifespan, and improved charge separation and transfer rates. Among inorganic oxide catalysts, CeO_2 has gained attention for its thermal stability, facile transition between Ce(IV) and Ce(III) oxidation states, substantial UV absorption, and enhanced electrical conductivity [11]. Especially, released oxygen acts as an oxygen carrier, crucial in oxidation reactions. Combining TiO_2 with CeO_2 enhances electron-hole pair separation and boosts photocatalytic activity. Recent studies have developed heterostructures using TiO_2 and CeO_2 as photocatalysts to optimize their functional properties [12].

In this study, a TiO_2-CeO_2 heterostructure was synthesized using a cost-effective hydrothermal technique, suitable for continuous industrial-scale production and environmental remediation applications. The photocatalytic activity of the TiO_2-CeO_2 heterostructure was examined with MB dye under visible light irradiation. Significantly enhanced photocatalytic activity was observed compared to pure TiO_2 nanoparticles.

2. EXPERIMENTAL DETAILS

2.1. Materials

Titanium(IV) butoxide ($Ti(C_4H_9O)_4$, 97.0%), Cerium(III) nitrate hexahydrate ($Ce(NO_3)_3.6H_2O$, 99.99%), Ammonium hydroxide (NH_3 in H_2O, 28%) were purchased from Sigma-Aldrich, Germany. Methylene Blue (MB, $C_{16}H_{18}ClN_3S$), Ethanol (C_2H_6O, 95%), Glycerol ($C_3H_8O_3$) were bought from AR Xilong, China. All chemicals used in the experiments had analytical purity grades without further purification.

2.2. Preparation of TiO_2 and TiO_2-CeO_2 heterostructure

In a standard procedure, the TiO_2-CeO_2 heterostructure composite was synthesized using the hydrothermal method [12]. Initially, 2 mL of titanium(IV) butoxide and 10 mL of glycerol were added directly to 60 mL of ethanol, and the mixture was stirred magnetically for 30 minutes at 250 rpm. Subsequently, the blended solution was transferred into a 100 mL hydrothermal autoclave reactor and maintained at 180 ^{0}C for 24 hours, followed by cooling to room temperature. The resulting samples were separated, washed multiple times with deionized water and ethanol, and then dried at 80 ^{0}C in an oven for 10 hours. In the next step, 3.0 grams of $Ce(NO_3)_3{\cdot}6H_2O$ were dissolved in 30 mL of deionized water, followed by 0.5 grams of the TiO_2 dispersed into the obtained solution. The pH value was adjusted to around 10 by adding ammonia solution, and the mixture was continuously stirred for 4 hours at ambient temperature. The solution was transferred to a 100 mL Teflon autoclave, held at 180 ^{0}C for 24 hours, and washed with deionized water and ethanol. The obtained products were dried for 24 hours at 80 ^{0}C under vacuum conditions and calcined for 3 hours at 500 ^{0}C with a heating rate of 5 ^{0}C /min.

2.3. Characterization of photocatalysts

The structural properties of the samples were investigated on the X-ray diffraction device D8 Advance Bruker (Germany) using Cu-kα radiation (geometry θ - 2θ and λ = 1.5418 Å). The FTIR was carried out to characterize the functional groups of the nanostructures using a Spectrum Two FT-IR DTGS instrument, model L1600400, serial number 102717, over the wavelength range of 400 - 4000 cm^{-1} at the Institute of Chemistry, Vietnam Academy of Science and Technology. The determination of the images and material structure was conducted through the employment of Transmission Electron Microscopes (TEM) using the JEM 1010 instrument from Japan, located at the National Institute of Hygiene and Epidemiology. The ultraviolet-visible (UV-Vis) absorption spectra were obtained in the wavelength range of 200 nm to 1000 nm using a Cary-60 UV-Vis spectrophotometer (American) at the Centre for Practice and Experiment, Vinh University.

2.4. Photocatalytic degradation studies

The photocatalytic activity was tested with MB, which is a common textile dye that appeared in the wastewater textile industry. Firstly, 50 mg of sample (TiO_2- CeO_2 heterostructure) was taken into a beaker and mixed with 100 mL of MB solution ($9{,}38.10^{-6}$ mol/L) at room temperature. Subsequently, the suspension was magnetically stirred in the dark for 60 minutes at 200 rpm until the catalyst system reached saturation. Then, the photocatalytic reaction was carried out under visible light irradiation (the spherical xenon lamp simulates the sun, AHD350W ultra-high pressure short). During the stirring, at various periods, approximately 5 mL of suspension was taken out, centrifuged at 10.000 rpm, stored in the dark, and measured the absorbance of the supernatant at a certain wavelength λ = 665 nm. For comparison, additional experiments are conducted under identical conditions using TiO_2 and without the heterostructure.

The removal efficiency (E (%)) of MB was calculated using:

$$E(\%) = \frac{C_0 - C_t}{C_0}.100\% \quad (1)$$

where C_0 and C_t are the concentration of the initial and remaining MB, respectively.

3. RESULTS AND DISCUSSION

3.1. Structural characterization

The crystallinity properties of the TiO_2-CeO_2 heterostructure is investigated by X-ray diffraction (XRD) technique and the result is illustrated in figure 1.

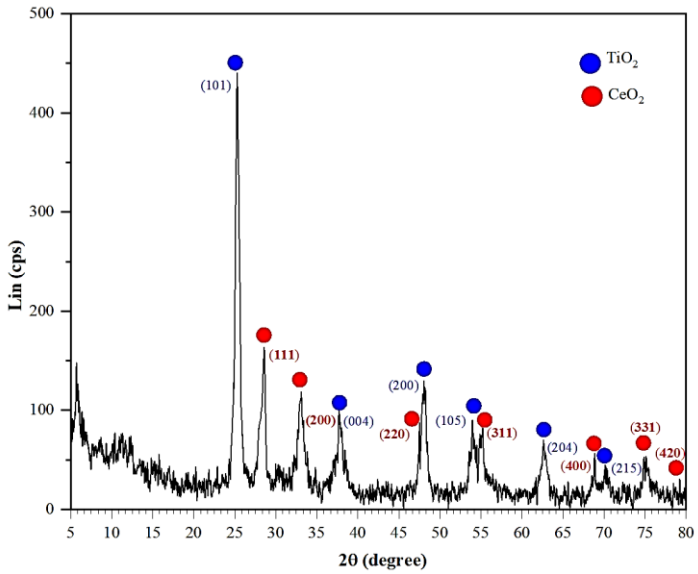

Figure 1. *XRD pattern of TiO_2-CeO_2 heterostructure.*

Firstly, the observed blue point diffraction peaks in the XRD pattern are well-matched with the anatase TiO_2 structure (JCPDS card no. 89-492 [13]), specifically on the (101), (004), (200), (105), (204), and (215) diffraction planes, showcasing high crystallinity of the (101) crystal surface in the TiO_2-CeO_2 heterostructure. Secondly, the red points in the XRD reveal distinct diffraction peaks on the (111), (200), (220), (311), (400), (331), and (420) diffraction planes of CeO_2 in the heterostructure (JCPDS No.75-8371 [14]), aligning with the pure cubic structure of CeO_2. No diffraction peaks of other species were detected, confirming the successful preparation of the TiO_2-CeO_2 heterostructure. Fan et al. [16] noted that the crystallinity of a TiO_2-CeO_2 heterostructure is lower than that of single-phase TiO_2 due to lattice distortion caused by differences in lattice

parameters between TiO_2 and CeO_2 crystals. Additionally, the CeO_2 peak in Fig. 1 is less sharp and prominent than that of TiO_2, indicating inferior crystallinity compared to TiO_2, supporting the findings of Meng et al. [16].

The average crystalline size of the TiO_2 and TiO_2-CeO_2 heterostructure was calculated using the Debye–Scherrer Equation (2) and was found to be 17.01 nm and 18.48 nm, respectively [15].

$$D = \frac{0.89.\lambda}{\beta.\cos\theta} \quad (2)$$

where D represents the estimated nanocrystallite size, λ is the wavelength of X-ray diffraction radiation in nanometers, θ is the diffraction angle, and β is the full width at half maximum (FWHM) of the (101) plane of anatase and the (111) plane of CeO_2.

3.2. FTIR spectrum analysis

The Fourier transform infrared technique was employed to investigate the chemical bonding in the TiO_2-CeO_2 heterostructure, as figure 2.

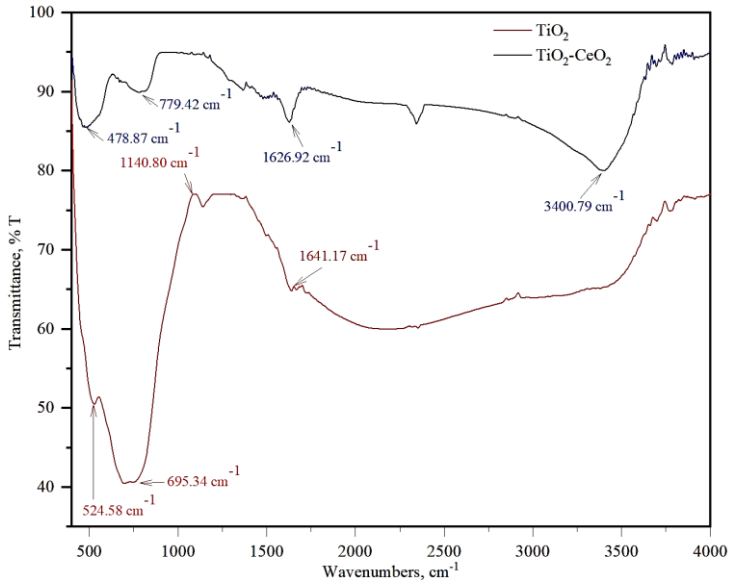

Figure 2. *FTIR spectrum of TiO_2 and TiO_2-CeO_2 heterostructure.*

The FTIR spectrum of TiO_2 can be observed in several peaks at 524.58 cm^{-1}, 695.34 cm^{-1}, 1140.80 cm^{-1}, and 1641.17 cm^{-1}. According to the standard spectra of TiO_2, the peaks at 524.58 cm^{-1} and 695.34 cm^{-1} are in the absorption range 450 - 800 cm^{-1}, which are attributed to the vibration of Ti-O bond in TiO_2 (anatase phase) lattice, it confirmes that the organic ligand was completely eliminated after calcined in a muffle furnace at 500 ^{0}C. The absorption peak of 1140.80 cm^{-1} could be the C-O vibration. The remaining peak of 1641.17 cm^{-1} was assigned to the bending vibration of water molecules absorbed on the surface of the materials [16]. Meanwhile, the spectrum of TiO_2-CeO_2 heterostructure showed some peaks at 478.87 cm^{-1}, 779.42 cm^{-1}, 1626.92 cm^{-1}, 2343.52 cm^{-1} và 3375.73 cm^{-1}, which identify the chemical bonds as well as functional groups in the compound. The intense bands at 478.87 cm-1 and 779.42 cm^{-1} are the fundamental stretching band (Ce-O) of CeO_2, which indicates the corresponding bands attributed to the metal-oxygen bond. The peak is around 650 cm^{-1} due to the stretching vibration mode Ti-O-Ti vibration superposed with the Ti–O–Ce of metal oxide [10]. The IR peak at about 1660-1600 cm^{-1} (peak at 1626.92 cm^{-1}) [14] can be assigned to the O-H bending vibrations of water molecules. The absorption bands seen at 3400.79 cm^{-1} could be attributed to the OH stretching vibration, meaning the sample is moist when measured [10].

3.3. Morphological characterization

Figure 3 illustrates the formation of the TiO_2-CeO_2 heterostructure, where TiO_2 nanoparticles are amalgamated with CeO_2, exhibiting a spherical shape with excellent dispersion and uniformity. Nevertheless, the resulting surface exhibits higher roughness and texture, primarily attributed to the deposition of CeO_2 nanoparticles onto the TiO_2 surface. The average size of the TiO_2-CeO_2 heterostructure is 21 nm, slightly larger than the pristine TiO_2, mainly due to particle aggregation, resulting in the formation of continuous clusters. This observation aligns with a study by M. Malekkiani et al., where TiO_2-CeO_2 particles, synthesized from TiO_2, displayed an average size of 27.93 nm [19].

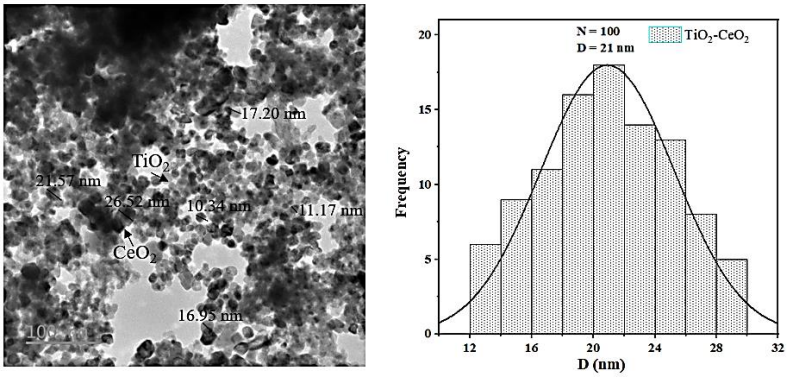

Figure 3. *TEM image of TiO_2-CeO_2 heterostructure.*

3.4. Photocatalytic activity

To investigate the absorption effect of MB, its degradation under visible light without using a catalyst was investigated, as shown in figure 4. The degradation efficiency of MB was 3,15% after light illumination for 120 minutes without a catalyst (control sample), and the photolysis of MB was negligible. TiO_2-CeO_2 provided a photodegradation efficiency of MB at 59.76% after 60 min of irradiation and practically 89.79% after 120 min, while TiO_2 produced a degradation efficiency of only 30.68% after 120 min of illumination. These results indicated that the TiO_2-CeO_2 heterostructure successfully improved the photodegradation capability of TiO_2 (an increase of over 59.11% when compared to the use of TiO_2 alone). The enhanced photocatalytic degradation of MB dye in a TiO_2-CeO_2 heterostructure solution is attributed to its high adsorption capacity, simultaneous adsorption of MB dye on TiO_2 and oxidation by hydroxyl radicals (OH*) on the conduction band of TiO_2 due to the contribution of CeO_2. Ce^{4+} species function as electron scavengers, capturing excited electrons from TiO_2, thereby retarding the recombination of electron-hole pairs (e^- - h^+ pairs) in TiO_2 and promoting the formation of superoxide anion radicals ($^*O_2^-$) and hydroxyl radicals OH*) on the surface of CeO_2 (figure 5).

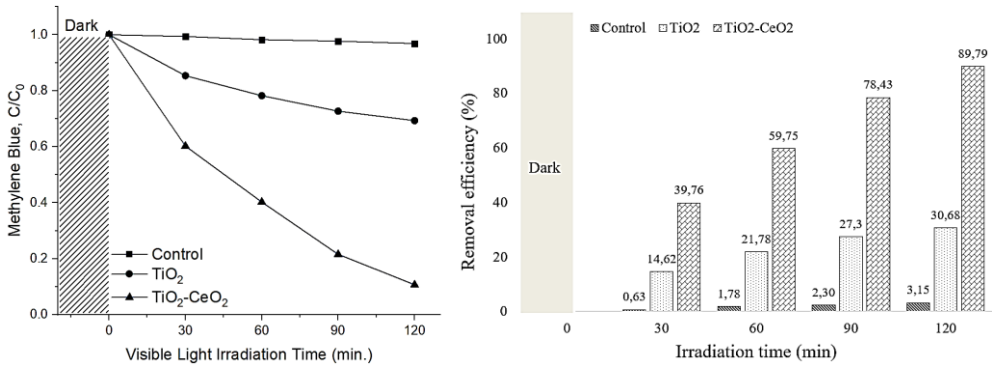

Figure 4. *The MB removal efficiency under visible light irradiation.*

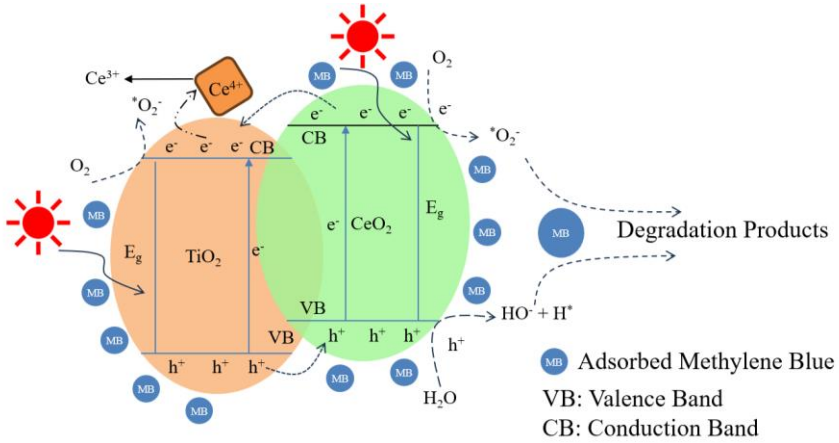

Figure 5. *Photocatalytic mechanism of TiO_2-CeO_2 heterostructure.*

4. CONCLUSIONS

Using a facile hydrothermal technique, a TiO_2-CeO_2 heterostructure was synthesized, and confirmed through XRD data, revealing the presence of anatase TiO_2 and cubic structures of CeO_2 in the material. The prepared TiO_2-CeO_2 heterostructure demonstrated excellent integration between TiO_2 and CeO_2, exhibiting an average size of approximately 21 nm with spherical shapes and uniform dispersion. When used as the photocatalyst, the TiO_2-CeO_2 heterostructure revealed quick and highly effective photodegradation of methylene blue with a removal percentage of 89.79% after 120 min of irradiating time. The superior photocatalytic performance of the materials is attributed to efficient photon-energy harvesting and enhanced charge separation. This is achieved through exciton-coupled charge transfer processes at the interfaces of the semiconductors TiO_2 and CeO_2, suppressing the recombination of electron-hole pairs in TiO_2 and promoting the formation of superoxide anion radicals ($*O_2^-$) and hydroxyl radicals ($^*OH$) on the surface of CeO_2. The heterostructure expands the light response range into the visible region, greatly improving visible light utilization, with potential applications in photocatalysis.

Acknowledgement: *This research was financially supported by the Ministry of Education and Training (MOET) under Project No. B2023-TDV-04.*

REFERENCES

[1]. B. Lellis, C. Z. Fávaro-Polonio, J. A.r Pamphile, J. C. Polonio, "*Effects of textile dyes on health and the environment and bioremediation potential of living organisms*," Biotechnology Research and Innovation,**Vol. 3**, No. 2, pp.275-290, (2019).

[2]. C. Chen, Z. Wang, S. Ruan, B. Zou, M. Zhao, F. Wu, "*Photocatalytic degradation of C.I. Acid Orange 52 in the presence of Zn-doped TiO_2 prepared by a stearic acid gel method*," Dyes and Pigments, **Vol. 77**, No. 1, pp. 204-209, (2008).

[3]. L. Maknun, Nazriati, I. Farida, N. Kholila, R.B. Muyas Syufa, "*Synthesis of silica xerogel based bagasse ash as a methylene blue adsorbent on textile waste,*" Journal of Physics: Conference Series, **Vol. 1093,** No. 1, pp. 1-5, (2018).

[4]. M. S. Mahmoud, J. Y. Farah, T. E. Farrag, "*Enhanced removal of Methylene Blue by electrocoagulation using iron electrodes*," Egyptian Journal of Petroleum, **Vol. 22**, No. 1, pp. 211-216, (2013).

[5]. S. R. Geed, K. Samal, A. Tagade, "*Development of adsorption-biodegradation hybrid process for removal of methylene blue from wastewater,*" Journal of Environmental Chemical Engineering, **Vol. 7**, No. 6, pp.1-20, (2019).

[6]. G. Fadillah, T. A. Saleh, S. Wahyuningsih, E. N. K. Putri, S. Febrianastuti, "*Electrochemical removal of methylene blue using alginate-modified graphene adsorbents*," Chemical Engineering Journal, **Vol. 378**, No. 12, pp. 122140, (2019).

[7]. N. Madkhali, C.Prasad, K. Malkappa, H. Y. Choi, V. Govinda, I. Bahadur, R.A. Abumousa, "*Recent*

update on photocatalytic degradation of pollutants in waste water using TiO_2-based heterostructured materials," Results in Engineering, **Vol. 17**, No.3, pp.100920, (2023).
[8]. D. Chen, Y. Cheng, N. Zhou, P. Chen, Y. Wang, K. Li, S. Huo, P. Cheng, P. Peng, R. Zhang, L. Wang, H. Liu, Y. Liu, R. Ruan, "*Photocatalytic degradation of organic pollutants using TiO_2-based photocatalysts: A review*," Journal of Cleaner Production, **Vol. 268**, No.9, pp. 121725, (2020).
[9]. D. Jiang *et al.*, "*A review on metal ions modified TiO_2 for photocatalytic degradation of organic pollutants*," Catalysts, **Vol. 11**, No. 9, pp.1039, (2021).
[10]. D T. M. Wandre, P. N. Gaikwad, A. S. Tapase, K. M. Garadkar, S. A. Vanalakar, P. D. Lokhande, R. Sasikala, P. P. Hankare, "*Sol-gel synthesized TiO_2-CeO_2 nanocomposite: an efficient photocatalyst for degradation of methyl orange under sunlight,*" Journal of Materials Science: Materials in Electronics, **Vol. 27**, pp. 825-833, (2026).
[11]. E. Kusmierek, *"A CeO_2 Semiconductor as a Photocatalytic and Photoelectrocatalytic Material for the Remediation of Pollutants in Industrial Wastewater: A Review,"* Catalysts, **Vol. 10**, No.12, pp.1435, (2020).
[12]. J. Wang, F. Meng, W. Xie, C. Gao, Y. Zha, D. Liu, P. Wang, "*TiO_2/CeO_2 composite catalysts: synthesis, characterization and mechanism analysis,*" Applied Physics A, **Vol. 124**, No. 645, pp.1-6, (2018).
[13]. N. Sofyan, A. Ridhova, A. H. Yuwono, A.Udhiarto, "*Preparation of anatase TiO_2 nanoparticles using low hydrothermal temperature for dye-sensitized solar cell*," IOP Conference Series: Materials Science and Engineering, **Vol. 316**, pp. 012055, (2018).
[14]. S. B. Khan, M. Faisal, M. M. Rahman, A. Jamal, "*Exploration of CeO_2 nanoparticles as a chemi-sensor and photocatalyst for environmental applications*," Science of The Total Environment, **Vol. 409**, No. 15, pp. 2987-2992, (2011).
[15]. Z. Fan, F. Meng, J. Gong, H. Li, Y. Hu, D. Liu, "*Enhanced photocatalytic activity of hierarchical flower-like CeO_2/TiO_2 heterostructures*," Materials Letters, **Vol. 175**, pp. 36-39, (2016).
[16]. A. O. Bokuniaeva, A. S. Vorokh, "*Estimation of particle size using the Debye equation and the Scherrer formula for polyphasic TiO_2 powder*," Journal of Physics: Conference Series, **Vol. 1410**, pp. 012057, (2019).
[17]. P. Praveen, G. Viruthagiri, S. Mugundan, N. Shanmugam, "*Structural, optical and morphological analyses of pristine titanium dioxide nanoparticles-synthesized via sol-gel route*," Spectrochimica Acta Part A: Molecular and Biomolecular Spectroscopy, **Vol. 117**, No.1, p. 622-629, (2014).
[18]. E. Wang *et al.*, "*Unique surface chemical species on indium doped TiO_2 and their effect on the visible light photocatalytic activity*," The Journal of Physical Chemistry C, 113(49), 20912–20917.
[19]. M. Malekkiani *et al.*, "*Fabrication of graphene-based TiO_2@CeO_2 and CeO_2@TiO_2 core–shell heterostructures for enhanced photocatalytic activity and cytotoxicity*," ACS Omega, **Vol. 7**, No. 34, pp.30601-30621, (2022).

TÓM TẮT

Tăng cường hoạt tính phân hủy quang hóa xanh methylen bằng hệ xúc tác dị thể TiO_2-CeO_2 dưới bức xạ ánh sáng khả kiến

Cấu trúc dị thể TiO_2-CeO_2 được tổng hợp bằng phương pháp thủy nhiệt đơn giản, có kích thước hạt trung bình 21 nm và có độ đồng đều cao so với các tiền chất thông thường. Các đặc trưng của chất xúc tác được xác nhận thông qua các kỹ thuật nhiễu xạ tia X (XRD), quang phổ hồng ngoại biến đổi Fourier (FTIR) và kính hiển vi điện tử truyền qua (TEM). Cấu trúc dị thể TiO_2-CeO_2 thể hiện hoạt tính quang xúc tác tốt hơn so với TiO_2 trong việc loại bỏ thuốc nhuộm xanh methylene (MB) dưới bức xạ ánh sáng khả kiến. Sự kết hợp của TiO_2-CeO_2 tạo ra các đường truyền điện tử, tạo điều kiện thuận lợi cho việc phân tách hiệu quả các cặp điện tử-lỗ trống và tăng cường hoạt động quang xúc tác của vật liệu. Cấu trúc dị thể TiO_2-CeO_2 thể hiện sự phân hủy quang nhanh và hiệu quả cao của xanh methylen, đạt tỷ lệ loại bỏ 89.79% sau 120 phút chiếu xạ. Hiệu suất này, cùng với việc tăng cường sử dụng ánh sáng khả kiến, gợi ý các ứng dụng rộng rãi trong lĩnh vực quang xúc tác.

Từ khoá: Hạt nano TiO_2; Cấu trúc dị thể TiO_2-CeO_2; Xanh methylene; Phân hủy quang xúc tác.